J Appl Electrochem (2011) 41:599–607
DOI 10.1007/s10800-011-0268-1

ORIGINAL PAPER

Study of electrochemical bleaching of *p*-nitrosodimethylaniline and its role as hydroxyl radical probe compound

Jens Muff · Lars R. Bennedsen · Erik G. Søgaard

Received: 9 April 2010 / Accepted: 17 February 2011 / Published online: 27 February 2011

Abstract In the present paper, research on the electrochemical bleaching of *p*-nitrosodimethylaniline (RNO) in different electrolyte systems is presented with special attention to the role of RNO as a selective hydroxyl radical probe compound. At a Ti/Pt_{90}–Ir_{10} anode, RNO was found to be bleached in 0.050 M sodium sulphate electrolyte due to lattice active oxygen without hydroxyl radicals being intermediately present. In 0.050 M sodium chloride, the bleaching rate was greatly enhanced due to indirect bulk oxidation by active chlorine species, again without the presence of hydroxyl radicals in the oxidation mechanisms. Under galvanostatic electrolysis, a linear relationship was found between the concentration of added chloride to a supporting sodium sulphate electrolyte and the first order rate constant of the bleaching reaction, showing the importance of the indirect bulk chlorine bleaching in chloride electrolyte systems. In this fashion both the chemically bonded active oxygen and the chemical bulk oxidation by active chlorine species proved to be valid bleaching pathways of RNO that according to these findings cannot be regarded as a fully selective hydroxyl radical probe compound. In addition, the difference in the mechanisms of chloride electrolysis at Ti/Pt_{90}–Ir_{10} and Si–BDD anodes was clearly demonstrated using *t*-BuOH as hydroxyl radical scavenger.

Keywords Electrochemical oxidation · Bleaching of dye · Hydroxyl radical probe compound · *p*-Nitrosodimethylaniline · RNO · *p*NDA · Chlorine oxidation

J. Muff · L. R. Bennedsen · E. G. Søgaard (✉)
Department of Biotechnology, Chemistry and Environmental Engineering, Aalborg University, Niels Bohrs Vej 8, 6700 Esbjerg, Denmark
e-mail: egs@bio.aau.dk

1 Introduction

The organic dyestuff *p*-nitrosodimethylaniline has been widely used in electrochemical oxidation literature as an easy detectable probe compound and spin trap for detection of particular hydroxyl radicals in aqueous oxidation studies. Qualitative and quantitative determination of the hydroxyl radical production is important as this very powerful oxidant is the key active species in a family of emerging environmental technologies known as advanced oxidation processes (AOPs). Due to higher treatment costs compared to conventional treatment techniques, AOPs are particular aimed for treatment of highly recalcitrant and non-biodegradable organic pollutants in soil, water, and air [1, 2]. Key AOPs include heterogeneous photocatalysis based on near ultraviolet (UV) or solar visible irradiation, alkaline ozonation, Fenton's or modified Fenton's chemistry, combinations of UV irradiation and chemical oxidants, and electrochemical oxidation. Direct detection of hydroxyl radicals is very challenging due to the extremely reactive nature of the radical. For that reason, indirect techniques are usually applied involving trapping of the hydroxyl radical by an addition reaction (spin trap) to produce a more stable radical (spin adduct) [3]. Spin trapping of hydroxyl radicals by 5,5-dimethyl-1-pyrroline *N*-oxide (DMPO) and detection by electron spin resonance (ESR) spectroscopy is a widely applied procedure, but this technique is not suitable for monitoring of larger flow systems and requires access to expensive analytical equipment. *P*-nitrosodimethylaniline (RNO, but also abbreviated *p*NDA in the literature), is an organic dye molecule that are easy detectable using UV–vis spectroscopy. With a system of well structured conjugated double bonds it has a strong absorption band in the visible region of the electromagnetic spectrum at 440 nm yielding a

strong yellow colour in aqueous solution. RNO has been a widely applied spin trap compound in several fields of chemistry, with the first study published in 1965 by Kraljic and Trumbore [4] on the use of RNO for the determination of relative rate constants for reactions of various solutes with hydroxyl radicals in experiments based on pulse radiolysis. A few years later, Baxendale and Khan [5] measured the absolute rate constant of the reaction between hydroxyl radicals and RNO to 1.25×10^{10} M^{-1} s^{-1}. The oxidation resulted in loss of absorption at the investigated 440 nm absorption band and followed second order kinetics. However, the decreased absorption was not permanent and showed an appreciable recovery. This was interpreted to be caused by dismutation of the oxidised RNO as showed in Fig. 1.

Since then, the bleaching of RNO has been reported to be very selective to oxidation by hydroxyl radicals, as it neither reacts with singlet oxygen ($^1O_2$), superoxide anions (O_2^-) or other peroxy compounds [3, 4, 6, 7]. The exact reaction mechanism of the oxidation is still unclear, and another more direct oxidation pathway has been suggested as well, where the hydroxyl radical directly attacks the nitroso group [8]:

$$\mathrm{RNO} + \mathrm{OH}^{\bullet} \rightarrow \mathrm{RNO}^{\bullet}\mathrm{OH} \quad (1)$$

During the last 15 years, electrochemical oxidation has been developed into a strong physico-chemical oxidation technique for degradation of organics in polluted water utilizing hydroxyl radicals, lattice active oxygen, and mediated bulk oxidation processes depending on the electrode material and process conditions used [9]. When aqueous solutions are passed through the electrochemical cell, the active oxygen species is produced at the surface of the anode from oxidation of water molecules, and these oxygen species are then capable of organic oxidation

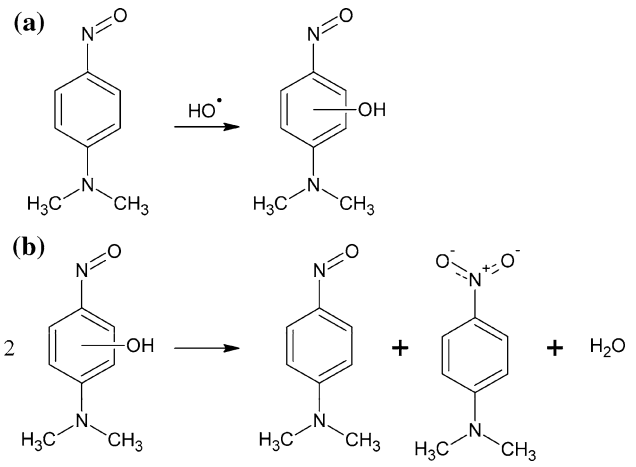

Fig. 1 Proposed mechanism of the oxidation of RNO by hydroxyl radicals. **a** Initial oxidation by $OH^{\bullet}$. **b** Dismutation of the oxidized intermediate. (Prepared after [5, 6])

leading to either partial oxidation or full mineralization. In electrochemical oxidation studies, the method of RNO bleaching has been adapted from the fields of medical chemistry [10–12], cell biology [6] and photobiology [4] as a tool for evaluation of the oxidation performance [3, 7, 8, 13–16]. RNO has in the electrochemical oxidation studies been used to obtain evidence for the presence of hydroxyl radicals in the studied systems. However, some discrepancies are found in the literature. RNO has by cyclic voltammetry been showed to be electrochemically inactive at Pt, IrO_2, SnO_2, and PbO_2 anodes [3, 13], but has as well been reported to be bleached in Ti/Pt and Ti/RuO_2 anode systems [16]. Ti/Pt and Ti/RuO_2 anodes represent types of anodes that according to the generally accepted models developed by Comninellis and co-workers [3, 9, 17], belongs to the class of active anodes that utilize chemisorbed lattice active oxygen, MO or MO_{x+1}, and not free hydroxyl radicals for organic oxidation. This is due to strong adsorption of the hydroxyl radical on these materials and hence further oxidation of the oxygen atom [9]. It could be an indication of that chemisorbed active oxygen as well may possess the ability of bleaching RNO. In addition, several electrochemical studies report bleaching of RNO by strong chemical oxidants as ozone [13] and chlorine [16] that can be generated during the electrochemical process and provide chemical bulk oxidation. In order to comply with the statements of hydroxyl radical selectivity, the bleaching due to these chemical oxidants was explained by an oxidation mechanism involving radical chain reactions generating hydroxyl radicals as the main intermediate oxidative agent [18–20]. At high pH, ozone oxidation has been proved to involve transient hydroxyl radicals [21], but the oxidation pathways proposed for active chlorine are more questionable and needs to be studied in greater detail, since oxidation of RNO by the active chlorine species themselves seems plausible and has formerly been indicated [16].

In the present study, the role of RNO as a fully selective hydroxyl radical probe compound has been studied in order to elucidate some of the presented discrepancies. The bleaching performance of RNO has been studied in an electrochemical oxidation system with different supporting electrolytes added, in order to assess the overall oxidation performance of the system. Special attention has been paid to sodium chloride electrolytes, where indirect bulk bleaching of RNO by electrolytic generated hypochlorous acid/hypochlorite (Eqs. 2–4) has been shown to happen in former research [16].

$$2\mathrm{Cl}^-(\mathrm{aq}) \rightarrow \mathrm{Cl}_2(\mathrm{aq}) + 2\mathrm{e}^- \quad (2)$$

$$\mathrm{Cl}_2(\mathrm{aq}) + \mathrm{H}_2\mathrm{O}(\mathrm{l}) \overset{K=4.4 \times 10^4 (25^{\circ}\mathrm{C})}{\rightleftharpoons} \mathrm{HOCl}(\mathrm{aq}) + \mathrm{Cl}^-(\mathrm{aq}) + \mathrm{H}^+(\mathrm{aq}) \quad (3)$$

$$HOCl\ (aq) \overset{pK_a=7.4(25^{\circ}C)}{\rightleftharpoons} OCl^{-}\ (aq) + H^{+}\ (aq) \quad (4)$$

Finally, a scavenging agent for hydroxyl radical removal has been used to investigate the proposed role of hydroxyl radicals in the indirect chlorine oxidation process to clarify the difference in bleaching pathways on Ti/Pt–Ir and BDD anodes.

2 Materials and methods

The investigation was performed in a batch recirculation experimental setup, where the RNO solution was pumped from a water cooled reservoir through the electrochemical cells at a flow rate of 430 L h^{-1} (Fig. 2), with the temperature kept constant at 20 ± 1 °C in all experiments. Two different commercial one-compartment electrochemical cells was applied (one at a time) in order to investigate different oxidation pathways. One was a cell of tubular design (sketched in Fig. 2a) from Watersafe S.A. (Greece) with an internal rod like anode of titanium coated with platinum alloyed with iridium ($Ti/Pt_{90}–Ir_{10}$) with a surface area of 60.3 cm^2. The cathode comprising the outer walls of the cell was a stainless steel 316 pipe with an internal diameter of 42 mm. The electrode gap in the cell was 6 mm. The second cell was a DiaCell type 100 cell (Fig. 2b) from Adamant Technologies S.A. (Switzerland) with 70.0 cm^2 silicon coated boron doped diamond (Si–BDD) anode and corresponding cathode mounted as plates with a 3 mm electrode gap in between.

During all experiments, the cells were operated at galvanostatic conditions at a current intensity of 1.9 A providing current densities of 32 mA cm^{-2} and 27 mA cm^{-2}, respectively. The initial concentration of RNO was 10 mg L^{-1} (6.7×10^{-5} M) with a total solution volume of 3.00 L. The investigated electrolytes were sodium sulphate, sodium nitrate, sodium chloride, and phosphate buffer systems (Na_2HPO_4, NaH_2PO_4, and Na_3PO_4) in concentrations from 0.001 to 0.154 M. All chemicals including RNO were of analytical grade and obtained from Merck and Sigma Aldrich. For the absorbance versus pH experiment, 0.1 M hydrochloric acid and sodium hydroxide solutions was used.

The bleaching of RNO was followed by spectrophotometric UV–vis absorbance measurements at the significant absorption band at 440 nm (Fig. 3) by a Varian Cary 50 UV–Visible Spectrophotometer. A linear correlation between RNO concentration and absorbance was found for the used concentration range as in accordance with Lambert–Beer ($\varepsilon_{440} = 3.3 \times 10^4$ L mol^{-1} cm^{-1}). Bulk oxidation and reduction potential (ORP), conductivity, temperature and pH were monitored with sensors in the reservoir.

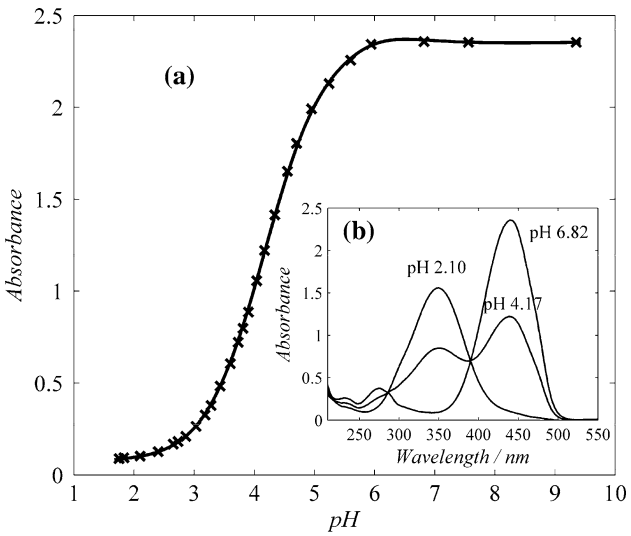

Fig. 3 **a** Absorbance of 10 mg L^{-1} RNO in 0.050 M Na_2SO_4 electrolyte at 440 nm versus change in pH. **b** UV–vis spectra of the 10 mg L^{-1} RNO in 0.050 M Na_2SO_4 electrolyte solution at three different pH values demonstrating the shift in maximum absorption band from 440 nm in the neutral/alkaline domain to 350 nm under acidic conditions

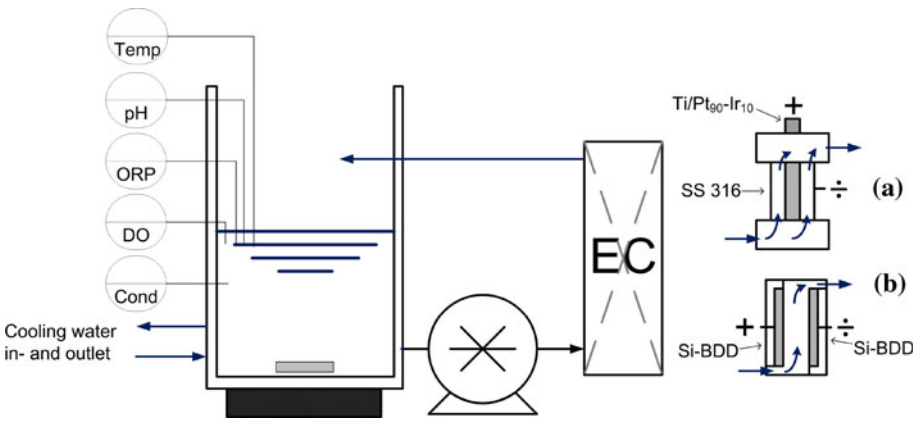

Fig. 2 The experimental setup based on batch recirculation from the water cooled reservoir. The basic design of the two applied electrochemical cells (EC); **a** Watersafe $Ti/Pt_{90}–Ir_{10}$ cell and **b** DiaCell type 100 Si–BDD cell

The reaction rate constant between RNO and hydroxyl radicals of 1.25×10^{10} M^{-1} s^{-1} is very large and well established [5, 22]. In order qualitatively to study the role of hydroxyl radicals in the system, tertiary butyl alcohol (*t*-BuOH) was added in excessive amounts of 0.10 M in order to scavenge the hydroxyl radicals according to the following competing reaction [22]:

$$(CH_3)_3COH + {}^{\bullet}OH \rightarrow {}^{\bullet}CH_2C(CH_3)_2OH + H_2O,\ k = 6.0 \times 10^8\ M^{-1}s^{-1} \quad (5)$$

The rate constant of Eq. 5 is 20 times less than *k* for the reaction with RNO, but the excessive initial amounts of *t*-BuOH compared to the initial RNO concentration of 6.7×10^{-5} M ensured a much more rapid initial reaction rate of the scavenging reaction compared to the RNO bleaching reaction.

3 Results and discussion

3.1 RNO absorbance versus pH by chemical adjustment

Most commonly, the studies of RNO bleaching has been performed in phosphate buffer systems, in order to keep constant pH during the electrolysis. However, this was not possible in all of the experiments in this study, since one of the aims was to study the bleaching performance in different electrolytes. The different electrolyte solutions resulted in changes of the solution pH during the experimental runs. For that reason as a preparative step to the electrochemical experiments, the absorbance of RNO in 0.050 M Na_2SO_4 at the absorption band at 440 nm was studied versus chemically changes in pH using drop wise addition of hydrochloric acid and sodium hydroxide (Fig. 3).

During the plain chemical pH adjustment, no influence was found on the RNO absorbance at 440 nm in the pH range from 6 to 12. Below pH 6, a reversible decrease in absorbance was seen, with the maximum absorption band gradually shifting to 350 nm found at strongly acidic conditions (pH 2.10). The reversible loss of absorbance at 440 nm due to the change in pH is proposed to represent the equilibrium reaction between the original and protonated RNO. The protons are proposed to interact with one of the lone pairs of the nitrogen atoms in RNO, either in the tertiary amine group or more in the nitroso group of RNO:

$$RNO(aq) + H^+(aq) \rightleftharpoons RNOH^+(aq) \quad (6)$$

Due to this, bulk pH was maintained above Eq. 6 in all of the electrochemical bleaching experiments, in order to secure that changes in absorbance at the 440 nm were due to electron transfer reaction. This was obtained by rare drop wise addition of 2 M NaOH when needed.

3.2 Electrochemical bleaching by surface and/or bulk oxidation

3.2.1 Bleaching in sulphate, nitrate, and phosphate electrolytes (surface oxidation)

The Watersafe cell with a $Ti/Pt_{90}–Ir_{10}$ anode represents the class of a primarily active anode and was used as the primary cell in the study in order to investigate if bleaching of RNO could be achieved also by MO active oxygen. The dynamically stable anode (DSA) type anodes represent the limiting case of active anodes producing MO with Si–BDD representing the limiting case of non-active anodes producing hydroxyl radicals [2]. Platinum based anodes are in between in sense of overpotential of oxygen evolution, but are closer related to the active anodes, and it has been convincingly showed by Jeong et al. [23] and others [24] that the production of hydroxyl radicals at Pt anodes is insignificant. At the $Ti/Pt_{90}–Ir_{10}$ anode material sulphate, phosphate, and nitrate anions can generally be considered as inert, and the bleaching in these supporting electrolytes seen in Fig. 4, reaching 70–80% absorbance removal in 4 h can be stated to be caused by oxidation of surface active oxygen species. This bleaching was a strong indication that RNO can be oxidized by MO too and not only hydroxyl radicals. The absorption spectra obtained in 0.050 M Na_2SO_4 are showed as an example in Fig. 5a.

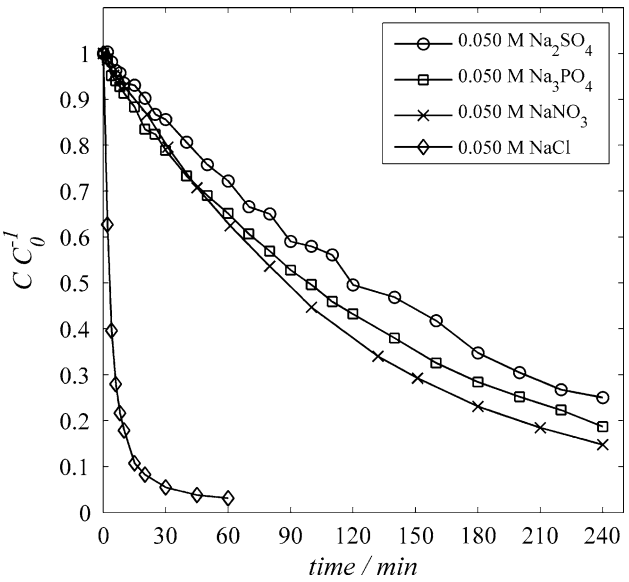

Fig. 4 Bleaching of 10 mg L^{-1} RNO in different supporting electrolytes at 32 mA cm^{-2} on $Ti/Pt_{90}–Ir_{10}$

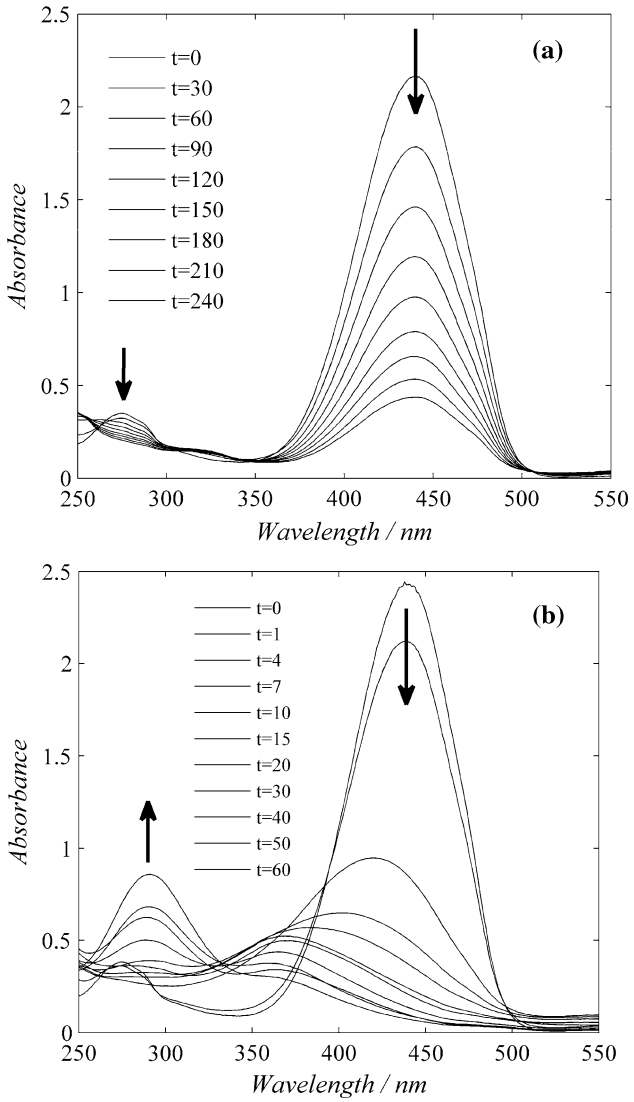

Fig. 5 UV–vis spectra obtained during bleaching of 10 mg L^{-1} RNO at 32 mA cm^{-2} on Ti/Pt_{90}–Ir_{10}. **a** supporting electrolyte: 0.050 M Na_2SO_4, and **b** supporting electrolyte: 0.050 M NaCl

The overall bleaching kinetics in these electrolytes followed first order kinetics consistent with mass transfer controlled bleaching, where the rate of oxidation at the fixed galvanostatic setting is determined by the rate of transport of organics to the anode surface and not the kinetics of the actual electrode reactions [9, 25]. This was expected and is usually seen in electrochemical batch recirculation systems operated under mass transfer controlled conditions, where the rate of oxidation at the fixed galvanostatic setting is determined by the rate of transport of RNO to the anode surface and not the kinetics of the actual electrode reactions [9, 25]. The bleaching rate could be sufficiently modeled by a first order equation:

$$\frac{d[\mathrm{RNO}]}{dt} = -k_{obs.} \cdot [\mathrm{RNO}] \tag{7}$$

The rate constant k_{obs} representing the overall bleaching rate was determined primarily by the mass transfer coefficient, k_m, of the cell. The rate constants obtained ($k_{obs.} = 9.67 \times 10^{-5}$–$1.35 \times 10^{-4}$ s^{-1}) were in the same order of magnitude as degradation rates of other aromatic organics reported in the literature [8, 15] and as the oxidation rates of the PAHs fluoranthene and pyrene obtained in the same setup at comparable current densities [26]. This showed that the initial oxidation of aromatic organics by the applied anode material was predominantly independent on the chemical nature of the molecules.

3.2.2 *Bleaching in sodium chloride with or without sodium sulphate supporting electrolyte (surface and bulk oxidation)*

In the sodium chloride electrolyte, the bleaching rate at the same constant current density was significantly increased. Chloride is an electroactive anion and will through (Eqs. 2–4) produce active chlorine species that contributed positively to the bleaching, probably caused by oxidation of the nitroso functional group:

$$\mathrm{R-NO(aq)} + \mathrm{OCl^-(aq)} \rightarrow \mathrm{R-NO_2(aq)} + \mathrm{Cl^-(aq)} \tag{8}$$

However, the specific site of attack on the RNO molecule by the chlorine species is unknown. The very fast initial bleaching rate showed a remarkable sluggish decay, when it reached 90% removal of the initial absorption. When the underlying UV–vis spectra were studied (Fig. 5b), it was evident that the oxidative action of active chlorine species in the chloride electrolyte produced intermediate oxidation products during the run, shifting the absorbance peaks to lower wavelength. The intermediate products were further degraded, but the spectral analysis at 440 nm measured the tailed absorbance of the intermediate peaks. The increasing absorption peak at 290 nm in Fig. 5b was identified to be caused by hypochlorite, which bulk concentration increased with time. The bleaching rate in the chloride systems, covering 90% bleaching, could be modeled by a pseudo-first order equation. Contained in the overall rate constant is the concentration of active chlorine, showed in Eq. 9 as the hypochlorite ion, that already in the first minutes was produced in excess amounts compared to the initial concentration of RNO.

$$\frac{d[\mathrm{RNO}]}{dt} = -k'_{obs.} \cdot [\mathrm{RNO}]\ ;\ k'_{obs.} = k \cdot [\mathrm{OCl^-}] \tag{9}$$

In the further data evaluation only the first 90% bleaching was considered.

The influence of chloride on the bleaching performance was investigated in more detail in a series of experiments, where increasing amounts of sodium chloride were added

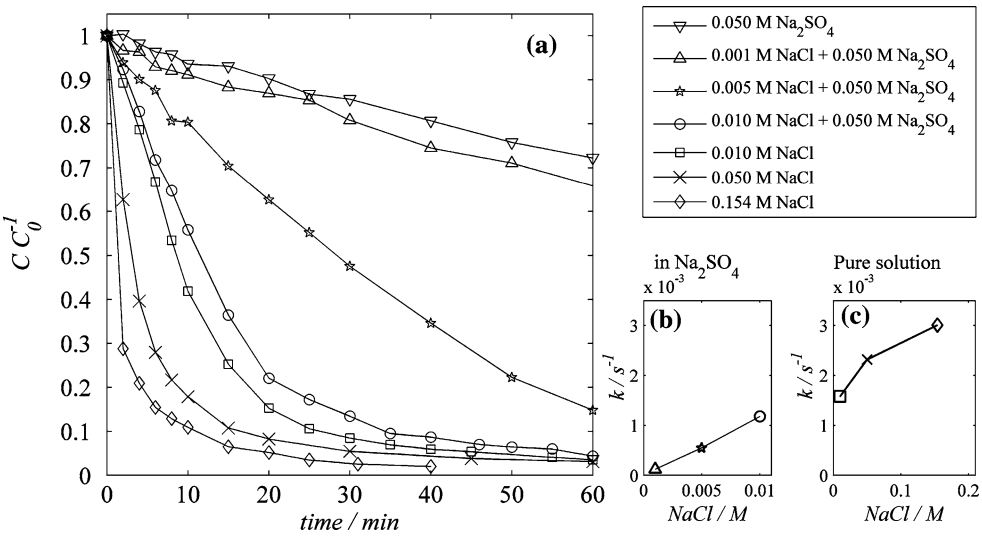

Fig. 6 **a** Bleaching of 10 mg L^{-1} RNO in NaCl electrolytes with and without supporting Na_2SO_4. **b** The first order rate constants of the bleaching versus the concentration of NaCl in supporting Na_2SO_4, and **c** the corresponding rate constants of the bleaching versus the concentration of NaCl

into a 0.050 M sodium sulphate supporting electrolyte with RNO. The bleaching curves obtained from the mixed electrolyte solutions showed that addition of 0.0010, 0.0050, and 0.010 M sodium chloride significantly enhanced the rate of oxidation compared to the bleaching baseline in pure 0.050 M sodium sulphate (Fig. 6a). The overall rate constants were linearly correlated with the added concentration of chloride (Fig. 6b). This could be explained by a linear correlation between the concentration of chloride in the electrolyte (up to a certain maximum) and the electrolytic active chlorine production [27]. Since all of the experiments were conducted at galvanostatic conditions with a current density of 32 mA cm^{-2}, the experiments clearly demonstrated the importance of the bulk active chlorine bleaching of RNO compared to the pure surface baseline bleaching.

In the single sodium chloride electrolytes a similar increase in bleaching rate was observed by increased chloride concentration. However, the same linearity was not followed and the increase in bleaching rate per mole of added chloride was much lower (Fig. 6c). In these experiments, the rate was limited by the applied current density.

When the bleaching rate in the single 0.010 M sodium chloride electrolyte ((○) Fig. 6a, b) was compared with a similar run, where 0.050 M sodium sulphate was added as supporting electrolyte ((□) Fig. 6a, c), it was higher in the pure system despite the lower ionic resistance in the mixed electrolyte system. The applied cell voltage in the pure system was high (17.8 V) compared to the mixed system (4.9 V), in order to reach the same operating constant current density of 32 mA cm^{-2}. Despite limited by this current density, the chloride oxidation was more efficient at the higher potential, comparatively faster, and yielded hypochlorite in larger quantities resulting in a higher bleaching rate. Even though being considered inert at the $Ti/Pt_{90}–Ir_{10}$ anode it cannot be completely excluded that oxidation of sulphate to persulphate or sulphate radicals did occur in minor extent when sodium sulphate was added as supporting electrolyte. This surface reaction could also become competitive to the chloride oxidation. Persulphate is a strong chemically oxidant such as chlorine, but despite the high standard reduction potential of this specie ($E_0 = 2.01$ V), the oxidation kinetics is usually very slow. In fact, a recent study of chemical oxidation of RNO by persulphate from our group has shown that no bleaching was observed without activation of persulphate for formation of sulphate radicals (Submitted). Electrochemical activation of persulfate through a one electron reduction at the cathode is a possible reaction that cannot be excluded either and needs to be studied in further detail. Another contributing factor to the decreased bleaching rate could be the increase in ionic strength caused by the sodium sulphate decreasing the activity of the chloride ions resulted in a slightly lower production rate of free chlorine. Finally, small amounts of ozone could be formed at the high cell voltage. Ozone has in a study by Wabner and Grambow [13] showed to be able to oxidize RNO, when produced electrochemically at lead dioxide and platinum electrodes.

3.3 Role of $OH^{\bullet}$ in surface and chloride mediated oxidation

Formerly, the oxidative mechanism of active chlorine bleaching of RNO has been proposed to be a radical chain reaction with hydroxyl radicals as the main oxidative species [20]. This proposal was based on a mechanism suggested by Epstein and Lewin [19] developed to describe the observed kinetics in bleaching of cotton by hypochlorite. In this mechanism, the reaction proceeded by a free radical chain reaction involving transient hydroxyl radicals with hypochlorous acid as the final product (Eq. 10):

$$\begin{aligned} &HOCl \rightleftharpoons OH^{\bullet} + Cl^{\bullet} \\ &Cl^{\bullet} + HOCl \rightleftharpoons OH^{\bullet} + Cl_2 \\ &Cl_2 + H_2O \rightleftharpoons HOCl + H^+ + Cl^- \end{aligned} \quad (10)$$

The initiating spontaneous cleavage of hypochlorous acid into chlorine and hydroxyl radicals lacked an explanation in this proposal and the pathway is considered questionable. Formation of a hydroxyl radical from hypochlorous acid will require a one electron reduction from a suitable electron donor [18]. Since the experimental setup is based on one-compartment cells it cannot be excluded that the reduction (Eq. 11) can occur at the cathode.

$$HOCl + e^- \rightarrow OH^{\bullet} + Cl^- \quad (11)$$

However, the main cathodic reaction seen in the experiments was incontestable hydrogen evolution from the water reduction reaction:

$$2H_2O + 2e^- \rightarrow H_2 + 2OH^- \quad (12)$$

3.3.1 *Chloride mediated bleaching in different pH domains*

In order to test the hypothesized reaction scheme in Eq. 10, chloride mediated oxidation of RNO was studied in two different pH domains of the conjugated active chlorine pair using phosphate buffer systems; pH 6, where hypochlorous acid was the predominant active chlorine species, and pH 10 with hypochlorite as the predominant species as according to Eq. 4. If the reaction scheme in Eq. 10 applies, hypochlorous acid was expected to be significantly more efficient for the bleaching reaction.

As seen in Fig. 7, the bleaching curves showed a similar exponential trend with a slightly higher rate constant for pH 6 ($k_{\cdot} = 1.9 \times 10^{-4}\ s^{-1}$) compared to pH 10 ($k_{\cdot} = 1.5 \times 10^{-4}\ s^{-1}$). This minor difference in reaction rate is believed to be explained by the higher standard reduction potential of hypochlorous acid ($E_0 = 1.48$ V) compared to hypochlorite ($E_0 = 0.81$ V). If the radical chain mechanism in Eq. 10 plays a role in chlorine bleaching, the difference in reaction rate was expected to be much higher.

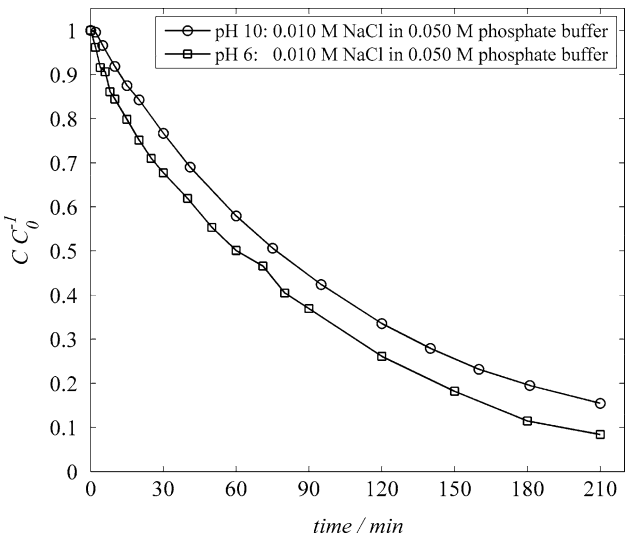

Fig. 7 Bleaching of 10 mg L^{-1} RNO in phosphate buffered NaCl electrolytes at pH 6 and 10, respectively

3.3.2 *Electrochemical bleaching of RNO in the presence of a hydroxyl radical scavenger*

For a qualitative study of the role of hydroxyl radicals in the investigated electrolyte systems, tertiary butyl alcohol (*t*-BuOH) was added in excess in order to remove all hydroxyl radicals if present, according to the competitive oxidation reaction (Eq. 5), and compare the bleaching rates with the similar non-scavenged systems. Experiments were performed in both sodium sulphate and sodium chloride electrolytes with both the Watersafe cell ($Ti/Pt_{90}–Ir_{10}$ anode) and the Diacell with the Si–BDD anodes. It is well established in the scientific community that BDD anodes produce significant amounts of hydroxyl radicals during water electrolysis [28], due to a larger electrochemical potential window than all other conventional anode materials. This non-active anode material was primarily introduced in the study in order to test and demonstrate the usability of excess *t*-BuOH amounts as competing hydroxyl scavenger.

The bleaching curves obtained with and without *t*-BuOH are seen in Fig. 8. At the $Ti/Pt_{90}–Ir_{10}$ anode, a very similar bleaching of RNO was found with and without the presence of 0.10 M *t*-BuOH in the 0.050 M sodium sulphate electrolyte (Fig. 8a). This complete independence of *t*-BuOH clearly demonstrated that no significant hydroxyl radical production occurred at the $Ti/Pt_{90}–Ir_{10}$ anode material and that the bleaching of RNO at the anode surface by this anode was entirely due to lattice active oxygen, MO. In the 0.050 M sodium chloride electrolyte 0.10 M *t*-BuOH did not too influence the bleaching rate by this material (Fig. 8a). This observation completely rejected the hydroxyl radical chain reaction proposal (Eq. 10) and stated that bulk RNO bleaching by active chlorine species entirely is due to the oxidative abilities of the hypochlorous acid/hypochlorite pair itself and not intermediate hydroxyl radicals.

At the Si–BDD anode, almost 80% bleaching was obtained within 120 min in the 0.050 M sodium sulphate electrolyte due to the increased hydroxyl radical production at this non-active anode and the higher bleaching efficiency of the radicals compared to the MO (Fig. 8b). Tertiary butyl alcohol did decrease the bleaching rate due to the competitive radical removal, but complete inhibition of

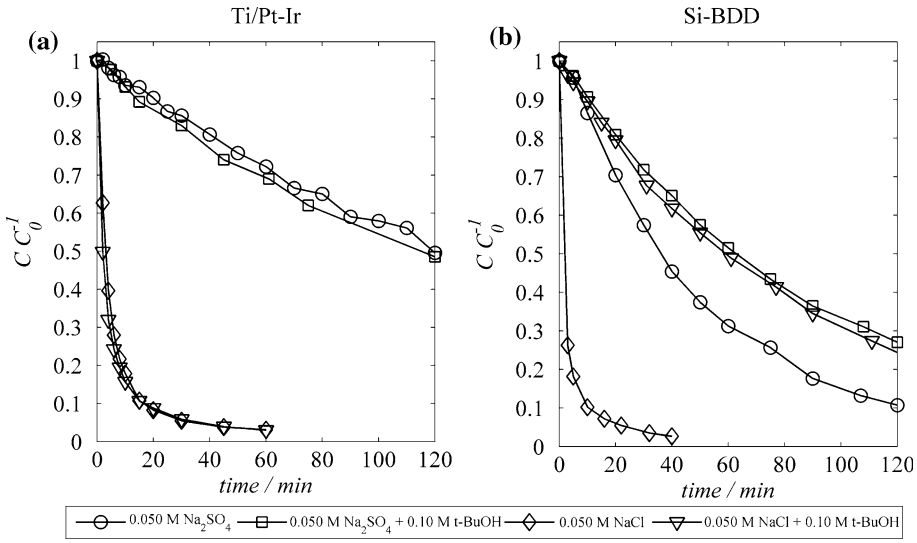

Fig. 8 Bleaching of 10 mg L^{-1} RNO by two different electrochemical cells in 0.050 M Na_2SO_4 and 0.050 M NaCl with and without the presence of 0.10 M *t*-BuOH as hydroxyl radical scavenger; **a** The Watersafe cell with Ti/Pt_{90}–Ir_{10} anode and **b** the DiaCell with Si–BDD anode

was not obtained. However, the experiment justified the use of *t*-BuOH as scavenging agent for the hydroxyl radical removal. The baseline bleaching of RNO was somehow surprising. One reason may be a direct oxidation of RNO at the diamond surface not mediated by the hydroxyl radicals, but a cyclic voltammetry study by Holt et al. [7] suggested that RNO was electrochemical inactive at this anode material. Another suggestion might be that the Si–BDD despite its classification as the limiting non-active anode material does produce some chemically bonded active oxygen not affected by the *t*-BuOH and capable of RNO bleaching as seen by the Ti/Pt_{90}–Ir_{10} anode. Additionally, sulphate can at BDD be oxidized into persulphate at the right conditions [29, 30]:

$$2SO_4^{2-} \rightarrow S_2O_8^{2-} + 2e^- \quad (13)$$

However, the electrosynthesis in Eq. 13 is mainly carried out in sulfuric acid solutions under carefully monitored conditions, and the RNO bleaching efficiency of persulphate is insignificant. Finally, reduction of RNO has in a study of photocatalytic bleaching of RNO been showed to be a fast pathway for color removal in aqueous solution [31]. In the one-compartment cell, reductive bleaching of RNO may be achieved at the Si–BDD cathode and can be the most likely candidate for the baseline bleaching.

The most distinct difference on the bleaching obtained with the two anode materials was observed in the sodium chloride electrolyte. The fast bleaching rate observed in 0.050 M sodium chloride ((◇) Fig. 8b) was completely reduced to the baseline bleaching ((▽) Fig. 8b) by the presence of *t*-BuOH. This observation clearly demonstrated that the electrolytic formation of active chlorine species at the BDD anode occurred through surface electrochemical reactions between the chloride ion and adsorbed hydroxyl radicals, forming adsorbed oxychloro species capable of bleaching RNO, a pathway formerly proposed the group of De Battisti [32]:

$$M(OH^{\bullet}) + Cl^- \rightarrow M(HOCl^{\bullet}) + e^- \quad (14)$$

In the presence of *t*-BuOH, the hydroxyl radicals were removed due to (Eq. 5) and the oxidation of chloride was inhibited. This was a clear distinction to the Ti/Pt_{90}–Ir_{10} anode that has high chloride affinity and the capability of direct electron transfer from the chloride ion to the anode forming the free chlorine species.

4 Conclusions

The electrochemical bleaching of *p*-nitrosodimethylaniline (RNO) in different electrolyte systems has been studied with special attention to the use of RNO as a selective hydroxyl radical probe compound. At Ti/Pt_{90}–Ir_{10}, RNO was found to be bleached in 0.050 M sodium sulphate electrolyte due to lattice active oxygen without hydroxyl radicals being intermediately present. In sodium chloride, the bleaching rate was greatly enhanced due to indirect bulk oxidation by active chlorine species, again without the presence of hydroxyl radicals in the oxidation mechanisms as formerly proposed by others. In this fashion both the chemically bonded active oxygen and the chemical bulk oxidation by free chlorine species proved to be valid bleaching pathways of RNO that according to these findings cannot be regarded as a fully selective hydroxyl radical probe compound. In addition, the difference on the mechanisms of active chlorine formation at Ti/Pt_{90}–Ir_{10} and Si–BDD anodes was clearly demonstrated using *t*-BuOH as hydroxyl radical scavenger.

Despite the lack of hydroxyl radical selectivity, RNO is a very applicable and easy to use compound for evaluation

of the overall electrochemical oxidation power in the design and optimization of electrochemical reactors, taking account of several oxidative species generated in the process.

Acknowledgments Financial support from the Danish Ministry of Science, Technology, and Innovation in the form of the Ph.D. study grant is gratefully acknowledged.

References

1. Mantzavinos D, Kassinos D, Parsons SA (2009) Water Res 43:3901
2. Comninellis C, Kapalka A, Malato S, Parsons SA, Poulios L, Mantzavinos D (2008) J Chem Technol Biotechnol 83:769
3. Comninellis C (1994) Electrochim Acta 39:1857
4. Kraljic I, Trumbore CN (1965) J Am Chem Soc 87:2547
5. Baxendale JH, Khan AA (1969) Int J Radiat Phys Chem 1:11
6. Bors W, Michel C, Saran M (1979) Eur J Biochem 95:621
7. Holt KB, Forryan C, Compton RG, Foord JS, Marken F (2003) New J Chem 27:698
8. Martinez-Huitle CA, Quiroz MA, Comninellis C, Ferro S, De Battisti A (2004) Electrochim Acta 50:949
9. Kapalka A, Foti G, Comninellis C (2008) J Appl Electrochem 38:7
10. Kunchandy E, Rao MNA (1990) Int J Pharm 58:237
11. Fitzl M, Suss R, Arnold K, Schiller J (2006) Chem Phys Lipids 140:11
12. Kaur IP, Geetha T (2006) Mini Rev Med Chem 6:305
13. Wabner D, Grambow C (1985) J Electroanal Chem 195:95
14. Feng C, Sugiura N, Shimada S, Maekawa T (2003) J Hazard Mater 103:65
15. Quiroz M, Reyna S, Sanchez J (2003) J Solid State Electr 7:277
16. Tanaka F, Feng CP, Sugiura N, Maekawa T (2004) J Environ Sci Health A Tox/hazard Subst Environ Eng 39:773
17. Bonfatti F, De Battisti A, Ferro S, Lodi G, Osti S (2000) Electrochim Acta 46:305
18. Holst G (1954) Chem Rev 54:169
19. Epstein JA, Lewin M (1962) J Polym Sci 58:991
20. Fukatsu K, Kokot S (2001) Polym Degrad Stab 72:353
21. Pi Y, Schumacher J, Jekel M (2005) Ozone Sci Eng 27:431
22. Buxton GV, Greenstock CL, Helman WP, Ross AB (1988) J Phys Chem Ref Data 17:513
23. Jeong J, Kim C, Yoon J (2009) Water Res 43:895
24. Canizares P, Martinez F, Diaz M, Garcia-Gomez J, Rodrigo MA (2002) J Electrochem Soc 149:D118
25. Martinez-Huitle CA, Ferro S (2006) Chem Soc Rev 35:1324
26. Muff J, Søgaard EG (2010) Water Sci Technol 61:2043
27. Muff J (2010) Ph.D. Thesis, Esbjerg Institute of Technology, Aalborg University, ISBN: 978-87-90033-71-2
28. Panizza M, Cerisola G (2009) Chem Rev 109:6541
29. Kraft A (2007) Int J Electrochem Sci 2:355
30. Serrano K, Michaud PA, Comninellis C, Savall A (2002) Electrochim Acta 48:431
31. Simonsen ME, Muff J, Bennedsen LR, Kowalski K, Søgaard EG (2010) J Photochem Photobiol A Chem 216:244
32. Bonfatti F, Ferro S, Lavezzo F, Malacarne M, Lodi G, De Battisti A (2000) J Electrochem Soc 147:592